AIAA SciTech Forum
23-27 January 2023, National Harbor, MD & Online
AIAA SCITECH 2023 Forum

10.2514/6.2023-2474

Transportation and Energy Ecosystem based on Martian Atmosphere

Miranda Anhalzer*, Alexis Abundio†, Johan Zambrano‡, Yusif Gurbanli ‡, and GeCheng Zha §
Dept. of Mechanical and Aerospace Engineering
University of Miami, Coral Gables, FL, 33124

Abstract

This paper conducts the preliminary feasibility study of a transportation and energy ecosystem based on Martian atmospheric conditions. The transportation system is to be realized by electric vertical takeoff and landing (eVTOL) air vehicles enabled by deflected slipstream with coflow jet (CFJ) to achieve ultra-high cruise lift coefficient and efficiency in the thin Martian atmosphere. The electricity will be provided by high-efficiency wind turbines with coflow jet blades to harvest energy from the Martian wind. The coflow jet active flow control is the key technology to tackle the low Reynolds number flows in the Martian atmosphere with high effectiveness, high efficiency, and low power requirement. Lithium-Sulfur batteries will be the eVTOL power and energy source. The wings are equipped with hydraulic systems for a folded wing mechanism to allow for transportation in the rocket fairing. The cruise Mach number of the aircraft is 0.35, with a cruise lift coefficient CL of 3.5, and the corrected lift-to-drag ratio including the CFJ power consumption, CL/CDc of 11.3. The vehicle mass is set to be 874.43 kg, with its low weight attributed to the use of a compact high lift CFJ system, high energy density batteries, and 12 lightweight propellers to power the flight mission. The aircraft has a range of 544.28 km, with an endurance of 1.44 hours. The wind turbine design has a hub height of 20 meters and a blade length of 5 meters with the targeted power efficiency of 55% or higher. An analysis of the potential wind power yield from the landing sites Utopia Planitia and Chryse Planitia supports the feasibility of the use of wind for energy production under Martian conditions. The Chryse and Utopia wind data analysis yielded results of an average daily energy production of 2.32 kWh, and 4.41 kWh respectively.

---

*Undergraduate Student, Department of Aerospace and Mechanical Engineering.
† Undergraduate Student, Department of Aerospace and Mechanical Engineering.
‡ Undergraduate Student, Department of Aerospace and Mechanical Engineering.
‡Undergraduate Student, Department of Aerospace and Mechanical Engineering.
§ Professor, AIAA Associate Fellow.

Nomenclature:

S Wing area
ρ free stream density
v_∞ Free stream velocity
q_∞ Dynamic pressure
S_1 front wing area
S_2 Rear wing area
c Chord length
b_1 Front wingspan
b_2 Rear Wingspan
AR Total aircraft aspect ratio
AR_1 Front wing aspect ratio
AR_2 Rear wing aspect ratio
$E_{uninstalled\ battery}$ Uninstalled battery energy
$m_{battery}$ Battery Mass
e Battery energy density
$E_{reserved}$ Reserved battery energy
N Number of propellers
A_{prop} Propeller area
D Propeller diameter
Pc_{Prop} Propeller power coefficient
T Thrust
P_{Prop} Propeller power
η Propeller efficiency
η_{drop} Propeller efficiency drop
P_{CFJ} CFJ Power
Pc_{CFJ} CFJ Power coefficient
$\eta_{CFJ-VTOL}$ CFJ VTOL efficiency
P_{hover} Hover power
$P_{prop-cruise}$ Propeller power at cruise
$P_{CFJ-cruise}$ CFJ power at cruise
η_{CFJ} CFJ efficiency
$P_{accesory-cruise}$ Accessory cruise Power
R Range
$Endurance_{cruise}$ Cruise endurance
$S1$ Wind speed with 1/7th power rule
$S2$ Wind speed at 5 meters
η_{WT} Wind turbine efficiency
P_{WT} Wind turbine Power

I. Introduction

To sustain human exploration and habitation on mars, a reliable transportation and energy system must be established. The Martian environment poses many limiting factors to the design and implementation of a successful Martian habitat. Due to a lack of infrastructure on the Martian surface, there is a need for the creation of a self-sustaining ecosystem on Mars, a transportation system, and an energy supply. Such an ecosystem can be achieved through harnessing Mar's natural resources. The development of large-scale road infrastructure on the Martian surface is preventively expensive. An economic transportation system to avoid roads on Mars is to fly with vertical takeoff and landing (VTOL). However, achieving flight on Mars has been deemed difficult because the Martian atmospheric density is only about 1/100 of Earth's [1].

The air vehicle, "Colibri", developed in this study is set to redefine the bounds of sustained flight on the Red Planet. With Co-Flow Jet technology, a super lift coefficient can be attained to maintain lift through flight and allow for VTOL capabilities. The aircraft power will be derived from the use of various batteries able to sustain the flight mission. The battery energy source will come from wind energy.

Presently, NASA's "Ingenuity" helicopter has been the only aircraft successful in achieving flight on Mars. The Ingenuity helicopter was able to achieve lift on mars mainly due to its low mass. Ingenuity has a total mass of 1.7 kg, with the ability to perform up to five 90-second flights [2]. The design and implementation of ingenuity as the first flying object on another planet marks significant scientific progress, however, further research and development must be done to allow for a future in Martian exploration. Helicopter flight on Mars for the high payload with human passengers is inefficient and difficult to operate. With Co-Flow Jet technology, sustained flights on Mars at low altitudes and VTOL abilities through the use of fixed, efficient wings are possible. The Colibri air vehicle concept adopted in this study is an electric VTOL (eVTOL) powered by batteries. The slipstream deflected from the propellers with 90-degree flow turning enabled by CFJ provides the high lift and efficiency required for both hover and cruise [3].

There have been some other studies detailing the use of CFJ technology for Martian aircraft. Mars Aerial Nuclear Global Landing Explorer (MANGLE) [4] is powered by nuclear energy and utilizes CFJ airfoils to sustain lift under Martian conditions. The nuclear reactor uses the carbon dioxide in the atmosphere as a propellant for the aircraft. The 899 kg design requires a max take-off power of 2.1 MW, and continuous power of 0.4 MW, flying at 0.41 Mach during cruise. This aircraft is primarily designed for the collection and transportation of soil samples. Even though the propulsion system of the MANGLE is not applicable to the proposed system of this study, its respective use of CFJ technology has implications for the Colibri design. Through the enhanced airfoil technology, a cruise lift coefficient of 3.5 is attained for the MANGLE.

With the eVTOL air vehicle system developed, the next critical issue is the energy source. Creating a self-sustainable energy ecosystem ensures the success of both the transportation system and future human habitation of Mars. To ensure the possibility of a successful flight mission for an eVTOL aircraft, extensive research and design needs to be done on viable energy options in a Martian setting. The creation of a successful ecosystem encapsulates a model where reliable energy sources produce enough energy that can be stored in batteries, and later be used for the aircraft transportation system. Martian atmospheric and weather conditions set certain limitations on the production of energy that is not applicable on Earth. The atmospheric composition of Mars inhibits the use of traditional combustion engines, as the oxygen composition on Mars is of negligible levels (.16% oxygen composition). Sustainable energy production systems can be implemented with the use of current and future technology. Historically, Martian technology has used both nuclear and solar systems for power production. The most recent rover mission (2020 Mission Perseverance Rover) relied on a radioisotope power system (RPS). The heat produced by plutonium

radioactive decay acted as the rover's "fuel". This Rover had a 4.8 kg power system, with capabilities of producing 110 Watts at optimal conditions [5]. RPS power systems have historically been the most common power system used for Martian rovers and explorers. This technology has been present in the Curiosity rover, the Viking 1 and 2 missions, as well as the Apollo missions on the moon. While RPS has proven to be reliable, there is a limit to the amount of energy that can be produced, with the energy output typically being capped at 1 kW [6]. Research has been conducted since then on the feasibility of fission surface power systems (FPSs). These systems have the potential to produce energy outputs of 1 kW to 1 MW. Most notably, NASA has completed on-earth testing of the Killopower system that was expected to produce 10 kWe per surface. This testing verified the surface fission system's ability to function safely and properly under both nominal and off-nominal conditions. Further testing on the moon is expected to occur within the next decay on NASA's current Fission surface power system project.

The use of photovoltaics for the harvesting of solar energy has also been used on previous NASA Martian missions. NASA's Mars pathfinder rover, ingenuity helicopter, and Exploration rovers have all used solar energy systems to power their respective missions. The use of solar power technology limited these rover missions around the equatorial region where the solar flux is at a maximum During prime mission conditions, the Mars exploration rover's solar arrays were able to harvest 900 Wh of energy per Martian sol [7]. These optimal energy productions occur only at specific sites under optimal solar flux conditions. Because the solar flux on Mars is 43.1% of that of earth, power outputs from solar arrays are drastically limited, thus limiting their ability to power complex Martian missions.

The dust storm on Mars provides a possibility of generating wind energy from Martian atmosphere. The harvesting of power from the wind has not been currently achieved on Mars. This is due to the significantly lower atmospheric density. Martian rovers have shown average wind speeds of 7-10 m/s occur in the northern hemisphere[8]. Conventional horizontal axis wind turbines at low Reynolds number have a power coefficient in the mid-30%. Conventional turbine efficiency values coupled with low surface density conditions on mars lead to a low threshold for power production on Mars. Wind turbines using CoFlow Jet blades at low Reynolds number is shown to increase power coefficient by 35% and more [9]. The use of CFJ integrated wind turbine blades has the potential to compensate for lower density values, allowing for sufficient power production under compromised conditions.

The purpose of this paper is to conduct a preliminary feasibility study to establish a transportation and energy ecosystem based on Martian atmosphere. The transportation is envisioned to be realized by CoFlow Jet eVTOL aircraft. The energy system is formed by wind energy harvested by high power CoFlow Jet wind turbines.

I.A. Co Flow Jet Integration

CFJ wings result in much more lift and reduced drag as compared to conventional wing configurations at low energy expenditure [9,10,11,12,13,14,15]. The penalty of increased lift in the form of induced drag is less for CFJ wings. The CFJ wings reduce pressure drag which results in higher aerodynamic efficiency [16]. Under Martian atmospheric conditions, ultra-high cruise lift coefficient must be achieved to allow for a fixed wing aircraft flight. This is necessary to compensate for the low air density on the Red Planet. Flow separation and stall for conventional aircraft airfoil designs limits the amount of lift that can be produced to have a compact size with minimum weight. The use of CFJ technology allows for ultra-high maximum lift coefficient [16, 17] and ultra-high cruise lift coefficient [18,19] with acceptable aerodynamic efficiency, thus allowing for eVTOL to be achieved on Mars.

As previously mentioned, the design of aircrafts able to sustain flight on Mars has been previously deemed improbable. A variety of limiting factors poses barriers to achieving this feat. Over the past two decades, much research has been published, making the flight on mars technologically feasible within the foreseeable future. With Co-Flow Jet technology, both sustained flights on mars at low altitudes and VTOL capabilities are possible. This is possible due to the CFJ's ability to produce a super lift coefficient by deflected slipstream [20, 19, 3].

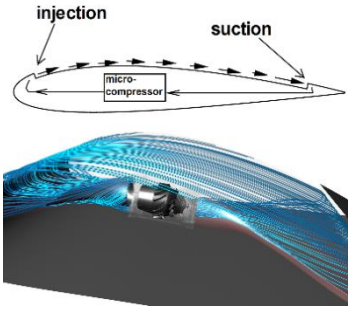

Figure 1. CFJ Injection and Suction [20,19,3]

The deflected slipstream enabled by CFJ allows for vertical take-off and landing without the need for rotor tilting mechanisms. By implementing CFJ technology in the flap of the airfoil, the necessary amount of lift needed for vertical take-off can be generated by deflecting the flap downwards. The slipstream can be turned 90deg downwards , converting the thrust produced by the propellers into vertical lift.[20, 3]

From our conceptual design study, a cruise lift coefficient of 3.5 is desirable and is thus used as the basis for the flight mission and aircraft sizing calculations. A cruise lift coefficient of 3.5 is very high and shows a significantly improved aerodynamic performance in comparison to traditional aircraft [21]. With a set cruise coefficient of 3.5, a take-off mass of 874.43 kg, and a total wing area of 12 m^2, the flight mission and aircraft sizing calculations were completed. Preliminary flight mission calculations were performed by using historical aircraft performance data, as well as CFJ aircraft research and wind tunnel testing. Detailed flight mission specifications can be seen in table 1.

II. Aircraft Design

II.A. Fuselage Design

The Aircraft fuselage was modeled after Jetson One eVTOL. Based on the Jetson One principal design, the original fuselage is suited for one passenger but was extended to accommodate two passengers. To minimize drag and increase aircraft flight efficiency, the fuselage is designed to accommodate two passengers in a tandem configuration. Using historical trends for subsonic aircraft the optimal fuselage diameter for a two-person aircraft was determined to be 1.64 meters, however, due to the passenger configuration, the fuselage diameter was reduced to 1.1 m [22]. Subsonic passenger aircraft usually have a fineness ratio of 0.08 to 0.125 [22]. There exists an optimum value of the fineness ratio at which the drag is minimized. For subsonic aircraft, this value is 0.3 but it is impossible to practically achieve this ratio for passenger aircraft. Hence, a fineness ratio of 0.10 is selected. Fuselage length can be calculated from the fuselage diameter and fineness ratio. With these values finalized as stated above, the fuselage length is calculated to be 8.5 meters.

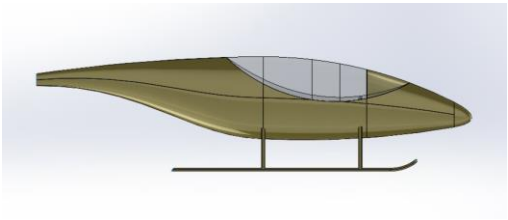

Figure 2. Fuselage and Landing Gear Assembly

Aircraft Flight Mission	
Range (km)	544.28
Cruise Mach	.35
Cruise Velocity (m/s)	104.77
TO Mass (kg)	874.43
Cruise Lift Coefficient	3.5
Cruise Drag Coefficient	.25
Max Power Required (kw)	354.37
Cruise Altitude (m)	3600

Table 1. Flight Mission Parameters

The aircraft sizing would allow for the aircraft to fit in the faring of the SpaceX Starship. The Starship fairing has an 8-meter diameter and an extended payload volume height of 22 meters [23]. This

rocket is set to be one of the most powerful to date, with plans to travel to both the moon and mars, making it the most feasible choice for the aircraft's transportation.

II.B. Landing Gear

The landing gear configuration was modeled after traditional landing systems for helicopters. Because of the aircraft's VTOL capabilities, the use of traditional retractable landing gear is not necessary. Wheel landing gears are not necessary and were decided against due to the inconsistency of the Martian terrain. A skid landing gear configuration was decided upon to allow for sufficient support for the large wingspans. The assembly of the landing gear and fuselage can be seen in figure 2.

II.C. Wing and Tail Design

To produce more lift efficiently, a tandem wing configuration was selected for wings. This configuration makes use of two wings and results in a reduction in drag while allowing duel lift vectors for stable hover performance. Using this aerodynamic specification, an 874.43 kg target mass for the aircraft, and a cruise lift coefficient value of 3.5, the specific sizing of the wings is calculated. For a tandem wing configuration, the following equations were used to calculate the wing areas for the aircraft.

$$S = 2\frac{W}{\rho c_{L,t} v^2} \tag{1}$$

The front-to-rear wing ratio ($\frac{S_1}{S_2}$) is set to have a value of .33.

$$S_1 = \frac{\frac{S_1}{S_2}}{\frac{S_1}{S_2} + 1} * S \tag{2}$$

$$S_2 = S - S_1 \tag{3}$$

With a chosen chord length of .65 meters, the respective wing spans of the aircraft can be calculated

$$b_1 = S_1/c \tag{4}$$

$$b_2 = S_2/c \tag{5}$$

Using the wing spans, the aspect ratios for the wings are calculated as seen below.

$$AR_1 = b_1^2/S_1 \tag{6}$$

$$AR_2 = b_2^2/S_2 \tag{7}$$

The total aspect ratio for the aircraft is found via the relation seen below.

$$AR = \frac{S_1 * AR_1 + S_2 * AR_2}{S_1 + S_2} \tag{8}$$

The following table presents the wing sizing parameters as calculated in the equations above.

Wing Parameters	**Front**	**Back**
Wing Area m^2	2.99	9.00
Wing Span m	4.61	13.85
Aspect Ratio	10.69	24.66
Chord m	.65	.65
Aircraft Parameters		
Total Wing Area	12	-
Total Aircraft Aspect Ratio	21.17	-

Table 3. Aircraft Mission Specifications

The wings are designed using the NACA 6421 airfoil. The hover lift for vertical takeoff and landing will be generated by simply deflecting the CFJ flap downward [20]. This would avoid the need to rotate the propellers or wings. This flap design would require chord of 60% of the chord length. The flap would be able to deflect downward at an angle of 90°.

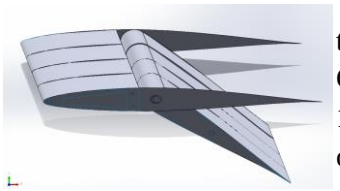

Figure 3. Wing and Aileron Model

The CFJ technology will be integrated into the wing which will be housed in the flap. A G8A micro-compressor was selected using previously performed CFJ research [24]. The injection slot of the duct will be placed at a height of 1.8% and a distance of 7.1% of the chord length of the flap. The suction slot of the duct will be at a distance of 83.2% chord length from the leading edge and a height of 0.6% the chord length of the aileron. Because the flap is the housing for the micro-compressor and duct that create the CFJ technology, the flap must be larger than a conventional aileron. As mentioned before, the aileron will be 60% the chord length of the entire wing. The front wing will be composed of 4 ribs, with 1.15 meters spacing between each rib. The rear wing is composed of 8 ribs, with 1.73 meters between each rib. The number of ribs was limited to 12 total to limit the total weight of the aircraft. A total of 12 micro compressors were selected in the design.

For aircraft having tandem wings with distributed propulsors and micro-compressors, horizontal and vertical stabilizers can be avoided. To limit the structure weight, a no-tail configuration is chosen for the aircraft. The reason is that the tandem wing design can provide pitching stability. The yaw and rolling stability can be controlled by the distributed propulsors and CFJ micro-compressors.

II.E. Power System and Battery

Battery electric power is used for propulsion. There are currently a variety of batteries available that have sufficient energy capacity to power short-term flights. One of the main obstacles in the Colibris design was finding a battery powerful enough to propel the aircraft in low-density conditions. It was also important to ensure that the energy density of the battery was high to limit the mass of the total aircraft assembly. Various battery options were considered including lithium-ion, lithium-sulfur, and novel lithium-oxygen batteries. With current commercially available technologies, the lithium-ion battery is the most

viable option (230-265 Wh/kg)[25]. These batteries' electric density specifications limit the range and endurance of the aircraft. However, as our design would be expected to be implemented in the future, lithium-sulfur batteries would be deemed more effective for our case. A well-respected "OXIS Energy" has already confirmed the availability of their 400 Wh/kg [Li-S] batteries. Their extrapolated rate of success predicts the 625 Wh/kg one to be available by 2026 [26]. Currently, power storage is one of the main limiting conditions not only for our project but the engineering world in general. As more advanced technologies become available, we would plan to stay up to and provide better parts for our aircraft while maintaining cost efficiency.

Another important aspect to keep in mind for batteries is their operational temperature range. As of right now, the Li-S batteries developed by OXIS are tested to work at temperatures around negative 60 to positive 85 ^{0}C [26]. The daily average temperature on Mars is considerably lower than on Earth (15 ^{0}C) being around -60 ^{0}C. Considering the typical daily Martian temperature ranges from -73 to +21 ^{0}C [27] , appropriate precautions must be considered for optimum aircraft performance. One option is to wait for the battery developer to enhance the lower boundary of the temperature range. Alternatively, the aircraft's internal environment control system can be further developed to assist with maintaining the micro-climate around the battery.

For the purpose of this feasibility study, it was decided to consider a lithium sulfur battery configuration with an energy density of 400 $\frac{Wh}{kg}$ (e), . With a battery mass of 193.5 kg, and an energy reserve of 20%, the following calculations are completed for further battery analysis.

$$E_{uninstalled\ battery} = \frac{e * m_{battery}}{1000} \tag{9}$$

$$Total\ available\ battery\ energy = E_{uninstalled\ battery} * (1 - E_{reserved}) \tag{10}$$

From the relations above, the uninstalled battery energy is found to be 77.40 kWh, and the total available battery energy is 61.92 kWh.

II.F. Power and Propulsion System

The following rotor performance metrics are selected and used for the propulsion system of the aircraft; these specifications were created using available data sheets from rotor manufacturers.

Specification	Performance
Dry Mass	13.0
Peak Torque	120 Nm
Continuous Torque	95 Nm
Optimal Operating Temperature	-40°-60° C
Take off system efficiency	94.5%
Cruise System Efficiency (⅓ Power)	95.7%

Table 4: Rotor Direct Drive Specifications [28]

The number of propellers selected for the design is derived using the following relations. The propeller diameter to chord ratio (D/c) is selected to be 2 and 2.5 for the front and rear wings respectively. With a wing chord length of .65 m, the diameter of the propellers is calculated

$$D_1 = \frac{D_{front\ prop}}{c} * c \tag{11}$$

$$D_2 = \frac{D_{back\ prop}}{c} * c \tag{12}$$

The number of propellers for each half of the front and rear wings is subsequently calculated using the wing spans.

$$N_{Front} = \frac{1}{2} * \frac{b_1}{D_1} \tag{13}$$

$$N_{back} = \frac{1}{2} * \frac{b_2}{D_2} \tag{14}$$

The above equations illustrate the minimum necessary number of propellers on each wing. With a chosen value of 12 micro compressors- 12 propellers are selected, with a 4-propeller configuration on the front wing and an 8-propeller configuration on the rear wing. This selection agrees with the propeller selection calculations done above.

The propeller area is calculated using the following values for the front and back wings, with N denoting the chosen number of propellers.

$$A_{prop} = N * \frac{\pi}{4D^2} \tag{15}$$

With a 12-propeller configuration, sufficient thrust to be produced for both hover and cruise conditions. The configuration of the rotor system consists of 8 rotors on the rear wing and 4 rotors on the front wing. Certain performance limitations must be considered due to the extreme weather conditions on Mars. When the temperature on Mars drops below -40 degrees Celsius, the performance of the rotors will drastically drop. Due to the operational temperature of the rotors, it is important to accurately measure and predict weather conditions when planning flight missions.

The freestream reference Mach used for the hover power calculations was .04 [29] Using the speed of sound on Mars (240 m/s), a velocity value of 11.97 m/s was obtained. The Martian atmospheric density for hover conditions was found to be .02 kg/m^3. With an aircraft aspect ratio of approximately 20, the power coefficient for the CFJ is found to be 3.20 [29]. Using this free stream velocity value, the CFJ power required, and actuator power required were calculated.

a. Hover Power:

The Power coefficient for the propeller is found using the reference free stream velocity, thrust (accounting for 1.18 multiplied by the aircraft's gross weight), wing area, and propeller area. Using the actuator disk theory, the propeller power coefficient is found. thrust of the

$$Pc_{Prop} = \frac{1}{q_\infty * v_{ref} * s}\sqrt{\frac{T^3}{2 * \rho * A_{prop}}} \tag{16}$$

The total propeller area for both the front and rear wing propellers is used.

The propeller power is calculated using the propeller efficiency with a value of .82, and an efficiency drop value of -0.1.

$$P_{Prop} = \frac{\frac{q_\infty * v_{ref} * s * Pc_{Prop}}{1000}}{\eta_{prop} + \eta_{drop}} \tag{17}$$

Using a power coefficient of 3.2, a CFJ micro compressor efficiency of .7, and a CFJ VTOL efficiency of .7, CFJ power required at hover is calculated.

$$P_{CFJ-hover} = \frac{\frac{q_\infty * v_{ref} * s * Pc_{CFJ}}{\eta_{CFJ}}}{\frac{1000}{\eta_{CFJ-VTOL}}} \tag{18}$$

From the Power calculated for the CFJ and propeller, the total Power required for take-off and landing conditions is found.

$$P_{hover} = P_{CFJ} + P_{Prop} \tag{19}$$

b. Cruise Power:

The cruise power is calculated using the propeller power required at cruise, the cruise CFJ power required, and the accessory power at cruise. The efficiencies used for the propeller and CFJ components are the same as seen above. The cruise CFJ power coefficient used is .052, with a cruise drag coefficient of .254, and a cruise velocity of 104.77 m/s.

$$P_{prop-cruise} = \frac{D * v_\infty}{\frac{\eta_{prop}}{1000}} \tag{20}$$

$$P_{CFJ-cruise} = \frac{q_\infty * v_\infty * s * Pc_{CFJcruise}}{\frac{\eta_{CFJ}}{1000}} \tag{21}$$

An accessory power value of .01 is considered in the following equation.

$$P_{accesory-cruise} = P_{accesory} * (P_{CFJ-cruise} + P_{prop-cruise}) \quad (22)$$

$$P_{cruise} = P_{accesory-cruise} + P_{CFJ-cruise} + P_{prop-cruise} \quad (23)$$

The following table presents the calculated power values at hover and cruise conditions.

Cruise Power	Power (kW)
$P_{prop-cruise}$	30.57
$P_{CFJ-cruise}$	7.3
$P_{accesary-cruise}$	0.38
$Total\ cruise\ power$	38.25

Table 5. Cruise Power Calculation

Hover Power	Power (kW)
$P_{prop-hover}$	353.13
$P_{CFJ-hover}$	1.35
$Total\ hover\ power$	354.37

Table 6. Hover Power Calculations

The hover time for the aircraft is 60 seconds, with 30 seconds for both the takeoff and landing portion of the mission. From this calculation the total energy required for takeoff and landing is 5.91 kWh. For a cruising time of approximately 1.44 hours, the energy required is 55.08 kWh. With an average climb power required of 21.41 kW and a climb and descent time of 68.2 seconds, the total energy expenditure for a single mission is calculated to be 61.8 kWh. The following section discusses the endurance and range calculations for the aircraft.

II.G. Range

The aircraft range and flight time are calculated using the total available battery energy and power parameters calculated for the flight mission.

$$Endurance_{cruise} = E_{battery}/P_{cruise} \quad (24)$$

$$R = \frac{(Endurance_{cruise} * 3600 * v_{\infty})}{1000} \quad (25)$$

The Colibri aircraft range is found to be 544.28 km, with a cruise time of 1.44 hours.

II.H. Weight analysis of Aircraft

Historical trends show the use of aluminum and steel as the major materials used for aircraft structures. However, ensuring a minimized weight when designing the aircraft was one of the most significant design constraints. Because of the low atmospheric density conditions of the Martian

atmosphere, it was imperative to limit the weight of the aircraft to ensure that enough lift could be produced throughout the flight mission.

The wing loading of the aircraft is used for the weight calculations for the aircraft. With the gravitational acceleration of mars (3.721 m/s^2), and a cruise lift coefficient of 3.45 the wing loading is calculated.

$$\frac{W}{s} = \frac{q_\infty * C_{Lcruise}}{g} \tag{26}$$

The gross mass of the aircraft is calculated using the relation below. With a structure factor (s) of .55, the structure mass and weight can be calculated.

$$m_{gross} = \frac{W}{s} * S \tag{27}$$

The weight of the CFJ micro-compressors is calculated using the CFJ power required at hover conditions and the power density of the micro compressors. The power density of the micro-compressors is 3 kw/kg.

$$m_{micro-compressors} = \frac{P_{CFJ-hover}}{Pd_{micro-compressors}} \tag{28}$$

The following table notes the weight calculations for the aircraft.

Weight Parameter	**Mass (kg)**	**Weight (lb)**
Battery	193.50	426.58
Structure	480.94	1060.27
Payload	199.99	440.90
Micro-compressors	0.45	0.99
Gross	**874.43**	**1927.76**

Table 7. Aircraft Weight

II.I Folding Wing Mechanism

Due to current payload fairing dimensions, a folding wing mechanism must be incorporated to allow for the aircraft to meet the dimensions requirements for transportation to mars. The SpaceX Starship rocket is chosen for the transportation of the aircraft Colibri due to its considerable fairing dimensions [23]. With a maximum diameter of 8 meters, a folded wing mechanism is necessary to fit the rear wing into the fairing. A simple linkage system was designed to allow for the rear wings to fold at 60 degrees. The wing is equipped with a double linkage system attached to the top of the wing via various shear clips. Hydraulic systems are equipped within each linkage system in the wing. The mechanisms is placed on both sides at a 5 meter distance from the fuselage, allowing for a 60-degree wing configuration to fit within the payload fairing of the rocket.

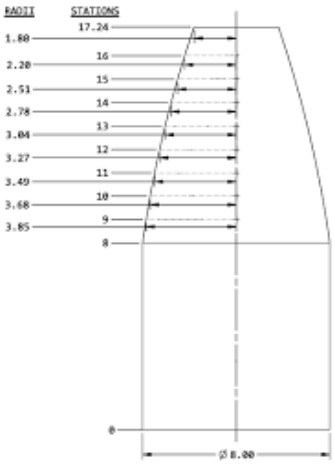

Figure 4. SpaceX Starship Payload Fairing Dimensions [23]

II.J Aircraft Performance and Mission Analysis

The above calculations and design parameters support the feasibility of a fully electric vertical takeoff and landing aircraft to be used under Martian conditions. With a total mission power requirement of 61.8 kWh, a range of 544.28 km, an endurance of 1.44 hours and a gross mass of 874.43 kg; the aircraft Colibri has the potential to become the first Martian aircraft. Aerial travel on mars can have considerable advantages within both fields of research and exploration. Longer range capabilities coupled with a notable increase in payload allowance could be vital in expanding our understanding of Mars and space.

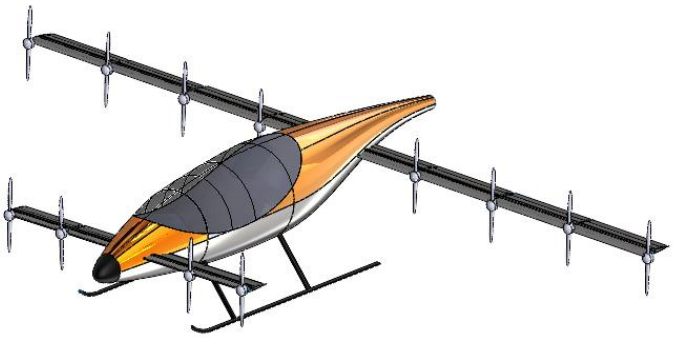

Figure 5. Martian eVTOL Colibri Aircraft Model

According to NASA, rovers are designed to travel approximately 100 meters per sol [30]. This is primarily due to the use of solar energy for power, with only a limited time per sol where solar irradiance is at its maximum, the rover is only able to travel during a four-hour period where the sun is at a peaked position. The Opportunity rover has had the longest driving distance than any other rover, achieving a lifetime range of 45.16 km over a period of 16 years [31]. With the Colibri aircraft, a range of 544.28 km is achieved, allowing for a 272.14 km mission (accounting for the aircrafts return to the base). With a single mission, the aircraft Colibri would be able to cover significantly more ground than has previously been achieved by all NASA Martian rover missions. Areas of Mars that have not yet been investigated, can be explored via the use of the eVTOL aircraft.

The payload capabilities for Martian exploration programs would also significantly improve with the use of a Martian aircraft. Due to the relatively small payload size of rovers, sample collection is significantly restricted. The samples collected by rovers are limited to rocks and soil using a process of sample caching. To date, space agencies have only been successful in sample retrieval for the moon, asteroids, and comets. There have been no samples received on earth from Mars. The ESA and NASA have been working on a Martian sample return mission where the perseverance rover is set to obtain 38 samples

which will be stored on mars and returned via later missions [32]. While a Martian sample-return mission has not succeeded to date, the possibility of the collection of larger samples can be made possible via the use of a larger vessel, such as the eVTOL aircraft Colibri. With a payload capability of 200 kg, the aircraft colibri has significant research advantages in comparison to that of current rovers.

III. Energy System

One of the largest barriers to executing a successful Martian system is sourcing enough energy to power the Martian mission. The ultimate goal of this feasibility study is to design a self-sufficient ecosystem that allows for sufficient energy to be produced, stored, and used for both the transportation system as well as for the future Martian colony. Various constraints limit possible energy sources on Mars. Various alternative renewable energy sources were considered in the feasibility study for the ecosystem. Three major energy systems were considered including the use of solar cells, nuclear fission, and wind power. Of these three it was concluded that the most promising energy-efficient results can be expected from the use of wind power technology. A detailed alternative analysis on potential energy sources can be found in the appendix.

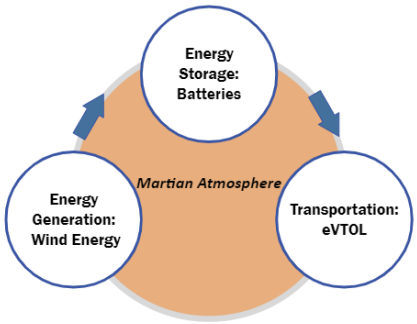

Figure 6. Diagram of Transportation and Energy Ecosystem Process

III. C. Wind Turbine

Wind power is proposed to be used specifically during compromised conditions- including instances of dust storms or reduced sunlight. Typical horizontal-axis wind turbines (HAWT) wind turbines regulate their efficiency at low wind speeds by varying their pitch angle. The angle of attack (AoA) of a wind turbine blade can be increased to increase wind turbine power output, however, this has its limitations as it needs to ensure that stall doesn't occur. With the Reynolds number on the Martian atmosphere being very low, these issues are exacerbated. The advanced CoFlow Jet 2-bladed HAWT are adopted in this study as the potential high power generation system. CFJ integration in wind turbine blades allows for lower pitch angles (higher AoA) to be achieved by increasing the stall margin [12]. This CFJ function allows for high wind turbine efficiency to be achieved, even under lower wind conditions where power output typically decreases. Using CFJ, increasing the AoA allows for wind turbine power output to be maximized at a much higher rate. This concept is similar to what is discussed in the context of the CFJ integrated aircraft wing. A preliminary study was conducted to compare wind turbine performance of the CFJ wind turbine in comparison to a baseline NREL turbine [12]. The turbine has a 10 meter diameter, and a hub height of 20 meters and is thus of suitable size to be carried as a full assembly inside the proposed rocket fairing. Further discussion on these proposed design dimensions can be found in the appendix. The study showed that the baseline turbine was able to achieve 36.3% efficiency at a speed of 7 m/s and a pitch angle of 3◦. The CFJ integrated wind turbine was able to increase the power output by 34% to a power coefficient of 49%[12]. There is room to further increase the power coefficient to 55% or higher.

The use of a CFJ integrated blade is essential for efficient power production under Martian low Reynolds number conditions. The CFJ's ability to have a significant increase in wind turbine efficiency makes the use of wind power on mars possible. Increased wind turbine efficiency has the potential to partially compensate for the lower density and Reynolds number values present on Mars.

III.C.1 Martian Wind Patterns

Wind power can be utilized for energy production on Mars. Despite Mars' density accounting for only 1/100 of that of earth, historical weather trends on Mars show promising data. The Martian wind patterns are still being studied today, but certain extrapolations can be made based on data collected by various Martian rovers. A preliminary analysis of Martian wind patterns in the northern hemisphere shows a yearly average wind speed varying from 7-10 m/s on the Viking 1 landing site [33]. These reported values show the average wind speed on mars at 1.6 m from the surface. While these wind speed values do have the potential to be sufficient for a wind turbine design, it is important to note that these wind values are limited to data collected from the Viking 1 rover. The Viking 1 site was chosen on the basis of mission safety. In addition to safety considerations, landing sites are also chosen on the basis of scientific and exploration data collection potential [46]. There is sufficient wind pattern research to show that higher surface wind speeds can be found in other areas. Atmospheric circulation models have been developed by researchers to show possible alternate locations where wind speeds are significantly higher [34]. These models are based on those done on earth with certain modifications made in lieu of differing geographical and topographical features between the two planets. Using areas showing high signs of wind erosion can indicate optimal wind turbine locations. Studies have suggested that sustained wind speed of up to 14 m/s can be achieved at a well-chosen site [34]. Models such as the ones described above can be used to predict wind speed in areas that have not been surveyed by current and past Martian rovers. Models have been created in the past to predict the winds above three possible landing sites at the northern summer solstice, showing estimated values for wind speed at a 1 km height from the surface. The wind speeds calculated were 20.9, 20.4, and 23.6 m/s [35]. The one-seventh wind profile power law can be used to estimate wind speeds at different heights from the surface. At 1.6 m the wind speed can be estimated to be 8 to 10 m/s. At a height of 15 m, the wind speed can be estimated to be 9.6 to 13.8 m/s[35]. This preliminary set of estimations shows that choosing an appropriate wind turbine location site can lead to increased wind speeds and subsequently an increased production of power. Sites with the potential to harbor faster wind speeds can include raised rim craters (where horseshoe vortices occur) and natural wind channels caused by geographical topography. These types of sites are typically used on earth to harbor faster wind speeds, so certain assumptions can be made for similar location selection on Mars. Raised rim craters with surrounding sand streaks can indicate optimal surface wind speed locations[35]. These sand streaks can be caused due to three-dimensional flow induced in the ambient wind flow by a perturbation with a small height to diameter ratio. Wind tunnel tests performed have been able to successfully reproduce similar sand streak patterns [35]. Showing that these patterns can potentially be used to verify the occurrence of three-dimensional flow around perturbance. There has been extensive research that shows that vortices form upstream of a crater when three-dimensional flow around protuberances occurs [35]. The formation of these vortices leads to a drop in ambient velocity leading to the vortices to converge downstream [35]. The convergence of these vortices downstream lead to an increased wind speed around the centerline of the wake. This increased speed is higher than that of the ambient speed. Strategic placement of wind turbine systems in areas with increased wind speed due to topographical features can potentially allow for maximum power energy output in wind turbines. It is important to thoroughly analyze Martian wind patterns as low Martian atmospheric density severely limits wind power production as opposed to what is possible on earth.

III.C.2 Wind Collection methodology

Further wind analysis was done analyzing wind potential across different topographical regions on the Martian northern hemisphere. An analysis was completed for the Utopia landing spot (Viking 2), the Chryse landing spot (Viking 1). The analysis for these two spots were selected on the basis of data availability. As previously mentioned, it is important to note that more favorable wind conditions may be possible in other regions of Mars. The following equations are used in wind energy production analysis for the three landing sites. The 1/7th wind power rule is considered when analyzing the wind speeds on the Martian surface to account for potentially higher wind speeds at higher heights. Considering a wind turbine height of 20 meters, an adjusted wind speed is calculated. A value of 5 meters is chosen for the wind measurement height.

$$S1 = S2 * \left(\frac{h1}{h2}\right)^{\frac{1}{7}} \tag{29}$$

The wind energy power calculations are completed considering a blade area of 78.54 m^2 , and an efficiency of 55%. The high efficiency is selected due to the use of CFJ integrated blades [12].

$$P_{WT} = \frac{1}{2}\rho A \eta_{WT} {S_{WT}}^3 \tag{30}$$

To ensure highest accuracy and reliability of processed data, the analysis was done using semi-hourly to hourly wind speed readings. Considering a Martian day is composed of 24.66 hours, approximately 25 wind data measurements were recorded on an hourly basis. Using the equations above, the hourly power and energy calculations were calculated and recorded. For daily energy values, every 25 consecutive hourly energy values were summed together. For weekly energy values, every 7 consecutive daily energy values were summed together. For monthly energy values, every 4 consecutive weekly energy values were summed together. It is important to note that Martian months are composed of 40-60 sols due to the eccentricity of Mars' orbit [45]. However, in order to maintain data analysis consistency in monthly energy calculations, it was decided to record the monthly readings every 4 weeks (28 days). Due to differing data availability, a varying number of sols were analyzed in each landing site analysis. The data sets used in both landing sites analyses averaged hourly wind speed measurements into 25 bins per sol [37,38]. The data sets used a cubic spline technique to interpolate values when data was missing in consecutive bins.

The following tables illustrate monthly energy production (calculated as described above) for each Martian location. The tables also denote energy production as a function of the number of wind turbines.

III.C.3 Chryse

The wind patterns on Chryse are analyzed using the data recorded by the Viking 1 lander. Data for a total 201 Sols was taken into consideration [37]. The Viking 1 lander recorded wind speed readings on an hourly basis, the subsequent power and energy calculations were calculated using the relations seen above.

Number of Wind turbines	1	2	3	4	5
Month	Energy (kWh) per Month				
1	38.55	77.11	115.66	154.21	192.76
2	14.33	28.66	42.99	57.32	71.65
3	10.23	20.46	30.69	40.92	51.15
4	25.79	51.58	77.37	103.16	128.95
5	226.19	452.38	678.58	904.77	1130.96
6	85.52	171.03	256.55	342.06	427.58
7	56.48	112.95	169.43	225.90	282.38
Average	**65.30**	**130.60**	**195.89**	**261.19**	**326.49**

Table 8. Chryse Energy Calculations

III.C.4 Utopia

The wind patterns on Utopia are analyzed using the Viking 2 lander data[36]. The Viking 2 data considered for this analysis was comprised of 567 sols. Within the data set used, there were approximately 25 wind speed measurements per day. The power was calculated using the wind speed readings on an hourly basis.

Number of Wind Turbines	1	2	3	4	5
Month	Energy (kWh) per Month				
1	16.25	32.49	48.74	64.99	81.23
2	14.89	29.77	44.66	59.54	74.43
3	19.01	38.02	57.03	76.04	95.05
4	19.44	38.88	58.31	77.75	97.19
5	62.24	124.47	186.71	248.95	311.18
6	89.36	178.71	268.07	357.43	446.79
7	87.70	175.41	263.11	350.81	438.51
8	221.16	442.31	663.47	884.63	1105.79
9	244.86	489.73	734.59	979.45	1224.32
10	333.32	666.63	999.95	1333.26	1666.58
11	76.97	153.94	230.91	307.88	384.85
12	27.04	54.08	81.12	108.16	135.20
13	4.54	9.08	13.63	18.17	22.71
14	11.24	22.47	33.71	44.94	56.18
15	11.63	23.26	34.88	46.51	58.14
16	39.18	78.35	117.53	156.71	195.89
17	330.69	661.38	992.07	1322.75	1653.44
18	170.68	341.37	512.05	682.74	853.42
19	339.76	679.53	1019.29	1359.06	1698.82
20	122.01	244.03	366.04	488.06	610.07
21	344.94	689.88	1034.81	1379.75	1724.69
Average	**117.94**	**235.88**	**353.82**	**471.77**	**589.71**

Table 9. Utopia Energy Calculations

III.C.5 Wind Energy Analysis

From the above tabulations for the Chryse, and Utopia landing sites wind data, extrapolations can be made on the use of wind energy in these locations. Using the comprehensive calculated energy data, it was deduced that Chryse and Utopia each yield an average daily energy production of 2.32 kWh, and 4.41 kWh respectively. With a Cruise power of 33.4 kW for a flight time of 1.44 hours, a hover power of 354.37 kW and a hover time of 60 seconds , and climb power of 21.41 kW with a climb time of 68.2 seconds, the total energy expenditure of a mission is calculated to be 61 kWh. With the lowest average monthly energy production being approximately 65.30 kWh, it can be deduced that with one to two wind turbines a monthly flight mission can occur. When considering the landing site of Utopia, with only one wind turbine, a flight mission could occur on a bi-weekly basis under favorable wind conditions. Even with the less favorable conditions found on Chryse, the use of two wind turbines would allow for at minimum a monthly flight mission. This analysis supports the possibility of using wind turbines to power an electric aircraft on mars. Furthermore, there are certain months of collected data that show a much higher energy production than that required for the aircrafts mission. External batteries can be used to store extra energy, which can then later be used under periods with unfavorable wind conditions.

When considering the use of multiple wind turbines, auxiliary power can potentially go to powering a Martian base, or support in the habitation of Mars. With the consideration that Martian mission energy requirements vary based on mission parameters and objectives, certain estimations have been made concerning the feasibility of Martian habitation projects. A study conducted by James et la. [34] performs an analysis on various energy expenditure estimations for Martian habitation. From this study, it is concluded that approximately 60 to 200 kW is necessary for a human Martian habitation mission. Using the CFJ wind turbine energy calculations seen above, it can be concluded that a small wind farm would not be sufficient to power a Martian outpost; however, with larger wind farms or potentially larger wind turbines, it is reasonable to assume that wind energy could be useful in the future.

Due to a limitation in available wind speed data, it would be reasonable to assume that a further understanding of wind speeds and potential wind energy production is possible in the future. The data as seen above does have certain limitations due to each of the landing sites data being of a different sample size. These wind results were also recorded at different times, and thus show that there is a possibility for data inconsistency. In addition to this, the data sets considered in this analysis did use a cubic spline technique to extrapolate values if data sets were missing. With these limitations considered, the results analyzed from the Viking lander 1 and Viking lander 2 still yield very promising data supporting the use of wind energy as an energy source on Mars. Further wind analysis can be found in the appendix.

IV. Conclusion

This paper conducts a preliminary feasibility study of a transportation and energy ecosystem based on Martian atmospheric conditions. The transportation system is to be realized by an electric vertical takeoff and landing (eVTOL) air vehicles enabled by deflected slipstream with coflow jet (CFJ) to achieve ultra-high cruise lift coefficient and efficiency in the thin Martian atmosphere. Via CFJ integration, the aircraft has a cruise lift coefficient of 3.5, with a corrected lift-to-drag ratio including the CFJ power consumption, CL/CDc of 11.3. The aircraft is powered by a Lithium-Sulfur battery with an energy density of 400 Wh/kg and a mass of 193.5 kg. With a cruise Mach number of .35, a high range of 544.28 km and an endurance of 1.44 hours, the eVTOL aircraft is shown to have promising performance parameters. The vehicle mass is set to be 741 kg, with 199.99 kg of available payload. The aircraft's low weight is attributed to the use

of a high lift CFJ system, high energy density batteries, and 12 lightweight propellers to power the flight mission. With a high range and payload capabilities, the aircraft Colibri has the potential to act as a transportation and surveying aircraft on mars.

Electricity will be provided by high-efficiency wind turbines with coflow jet blades to harvest energy from the Martian wind. Based on the wind analysis performed, it was concluded that with a CFJ integrated wind turbine, sufficient wind energy can be produced to power the aircrafts mission. Martian wind pattern analysis was conducted on the Utopia and Chryse landing sites to show the feasibility of the use of wind turbines to power the aircraft. From the analysis it was found that even under the weakest wind speed conditions, a small number of wind turbines have the capability to power one to two flight missions per month. From this analysis it is concluded that the transportation and energy ecosystem is a viable project for exploration and transportation on Mars. The aircrafts high range and reasonable mission power requirements of 61.8 kWh, coupled with sufficient energy yield from CFJ integrated wind turbine, support the feasibility of a the eVTOL transportation and energy ecosystem based on a Martian atmosphere.

References

[1] NASA. (n.d.). *Mars atmosphere model - metric units*. NASA. Retrieved May 29, 2022, from https://www.grc.nasa.gov/www/k-12/airplane/atmosmrm.html
[2] NASA. (n.d.). *Mars helicopter*. NASA. Retrieved May 29, 2022, from https://mars.nasa.gov/technology/helicopter/
[3]Warwick, G., "CoFLow Jet Moves to Develop Deflected-Slipstream eVTOL", Aviation Week, Advanced Air Mobility Report, March 9, 2022]
[4]Sterling, R. W and Zaki, R. A. and Wang, Y. and Agreda, R. A. and Zha, G.-C, "Mars Robotic Global Exploration Network", AIAA Paper 2016-5600, AIAA SPACE and Astronautics Forum and Exposition 2016, Long Beach, CA, 13-16 September 2016
[5]NASA. (n.d.). *Electrical power*. NASA. Retrieved May 29, 2022, from https://mars.nasa.gov/mars2020/spacecraft/rover/electrical-power
[6]Furlong, R. R., & Wahlquist, E. J. (2000). 00/00199 U.S. space missions using Radioisotope Power Systems. *Fuel and Energy Abstracts*, *41*(1), 21. https://doi.org/10.1016/s0140-6701(00)87610-9
[7]Hess, S. L., Henry, R. M., Leovy, C. B., Ryan, J. A., & Tillman, J. E. (1977). Meteorological results from the surface of Mars: Viking 1 and 2. *Journal of Geophysical Research*, *82*(28), 4559–4574. https://doi.org/10.1029/js082i028p04559
[8] Williams, D. R. (n.d.). Mars fact sheet. NASA. Retrieved May 29, 2022, from https://nssdc.gsfc.nasa.gov/planetary/factsheet/marsfact.html
[9] Yan Ren, Paula Alejandra Barrios, Gecheng Zha, "Simulation of 3D Co-Flow Jet Airfoil with Integrated Micro-Compressor Actuator", AIAA Paper-2022-3553, AIAA AVIATION Forum, June 27-July 1, 2022, Chicago, IL & Virtual
[10] Paula A. Barrios, Yan Ren, GeCheng Zha, "Design of High Width-Diameter Ratio Injection and Suction Ducts for Co-Flow Jet Airfoil", AIAA Paper-2022-3772, AIAA AVIATION Forum, June 27-July 1, 2022, Chicago, IL & Virtual
[11] Kewei Xu, Gecheng Zha, "3D Aircraft Control Surface Enabled by Co-Flow Jet Flap", AIAA Paper-2022-3889, AIAA AVIATION Forum, June 27-July 1, 2022, Chicago, IL & Virtual
[12] Yan Ren, Kewei Xu, and Gecheng Zha, "Wind Turbine Effciency Enhancement by CoFlow Jet Airfoil", AIAA Paper 2022-1787, AIAA Scitech Forum, January 3-7, 2022, San Diego, CA & Virtual
[13]Yan Ren, Gecheng Zha, "Performance Enhancement by Tandem Wings Interaction of CoFlow Jet Aircraft", AIAA Paper 2021-1823, AIAA SciTech Forum, 11–15; 19–21 January 2021, VIRTUAL EVENT

[14] Yang Wang, Gecheng Zha, “Study of Mach Number Effect for 3D Co-Flow Jet Wings at Cruise Conditions”, AIAA Paper 2020-0045, AIAA SciTech Forum, 6-10 January 2020, Orlando, FL
[15] Purvic Patel, Hong-Sik Im, Gecheng Zha, “Numerical Investigation of Non-Synchronous Vibration with Fluid-Structure Interaction using Delayed Detached Eddy Simulation”, AIAA Paper 2020-0384, AIAA SciTech Forum, 6-10 January 2020, Orlando, FL
[16] Yunchao Yang, Gecheng Zha, "Super-Lift Coefficient of Active Flow Control Airfoil: What is the Limit?", AIAA Paper 2017-1693, AIAA SCITECH2017, 55th AIAA Aerospace Science Meeting, Grapevine, Texas, 9-13 January 2017
[17] Gecheng Zha, Yunchao Yang, Yan Ren, Brendan McBreen, " Super-Lift and Thrusting Airfoil of Coflow Jet Actuated by Micro-Compressors ", AIAA Paper-2018-3061, AIAA AVIATION Forum 2018, 2018 Flow Control Conference, June 25-29, 2018, Atlanta, Georgia
[18]Jaehyoung Jeon, Yan Ren, Gecheng Zha, "Toward Ultra-High Cruise Lift Coefficient Using 3D Flapped CoFlow Jet Airfoil", Proceedings of 2023 AIAA SciTech Forum 23–27 January 2023National Harbor, MD
[19]Jaehyoung Jeon, Brendon McBreen, Yan Ren, Gecheng Zha, "Study of 3D Flapped CoFlow Jet wings for Ultra-High Cruise Lift Coefficient", Submitted to 2023 AIAA Aviation and Aeronautics Forum, June 12-16, 2023, San Diego, CA
[20]Ren. Y. and Zha, G.-C., "Simulation of 2D CoFlow Jet Deflected Slipstream VTOL Transition Transient Flows", 10th Annual Electric VTOL Symposium, Mesa, AZ, Jan. 24-26, 2023
[21] Liu, Z., & Zha, G. (2016). Transonic airfoil performance enhancement using co-flow jet active flow control. *8th AIAA Flow Control Conference*. https://doi.org/10.2514/6.2016-3472
[22] Corke, Thomas C., Design of Aircraft; Prentice Hall, 2003
[23]SpaceX. (2020). *Starship Users Guide*. SpaceX.
[24] Paula A. Barrios, Yan Ren, Kewei Xu, GeCheng Zha, “ Design of 3D Co-Flow Jet Airfoil with Integrated Micro-Compressor for High Operating Efficiency at Cruise Condition”, AIAA Paper 2021-2581, AIAA AVIATION Forum, August 2-6, 2021, VIRTUAL EVENT
[25] Lithium-Ion Battery. Clean Energy Institute. (2020, September 25). Retrieved from http://www.cei.washington.edu/education/science-of-solar/battery-technology/
[26] Li, Shuli & Lin, Zhan. (2015). Lithium-Sulfur Battery. Green Energy and Technology. 172. 587-610. 10.1007/978-3-319-15458-9_21.
[27] US Department of Commerce, N. O. A. A. (2022, November 29). The planet Mars. National Weather Service. Retrieved from https://www.weather.gov/fsd/mars#:~:text=Mariner%204%2C%20which%20flew%20by,%2C%20to%20%2B70%20degrees%20F.
[28] H3X. (n.d.). HPDM-250 Datasheet. Retrieved May 29, 2022. H3X.
[29] Gecheng Zha, Yan Ren, Jiaye Gan, Daniel Espinal, “A High Efficiency Low Noise VTOL/ESTOL Concept Using CoFlow Jet Airfoil”, AIAA Paper 2019-4467, AIAA Propulsion and Energy 2019 Forum, 19-22 August 2019, Indianapolis, IN
[30] NASA. (n.d.). Moving around Mars. NASA. Retrieved from https://mars.nasa.gov/mer/mission/timeline/surfaceops/navigation/#:~:text=Although%20the%20rover%20is%20capable,feet)%20in%20a%20single%20sol.
[31] NASA/JPL-Caltech. (n.d.). Driving Distances on Mars and the Moon. NASA Science Mars Exploration Program. Retrieved from https://mars.nasa.gov/resources/6471/driving-distances-on-mars-and-the-moon/
[32] NASA. (2022, July 27). NASA Will Inspire World When It Returns Mars Samples to Earth in 2033. Perseverance Mars Rover. Retrieved from NASA Will Inspire World When It Returns Mars Samples to Earth in 2033.
[33] Hess, S. L., Henry, R. M., Leovy, C. B., Ryan, J. A., & Tillman, J. E. (1977). Meteorological results from the surface of Mars: Viking 1 and 2. *Journal of Geophysical Research*, *82*(28), 4559–4574. https://doi.org/10.1029/js082i028p04559

[34] James, G., Chamitoff, G. E., & Barker, D. (1998). Chapter 12 POWER ON MARS. In *Resource utilization and site selection for a self-sufficient Martian outpost*. Houston, TX: National Aeronautics and Space Administration, Lyndon B. Johnson Space Center.
[35] Haslach, H. W. Jr., "Wind Energy: A Resource for a Human Mission to Mars," Journal of the British Interplanetary Society, Vol. 42, No. 4, April 1989, pp. 171-178.
[36] Tillman, J. E., & Johnson, N. C. (1997, June 19). Viking Lander 2 Binned and Splined data. Retrieved from https://www-k12.atmos.washington.edu/k12/mars/data/vl2/part5.html.
[37] Murphy, J. R., Leovy, C. B., & Tillman, J. E. (97AD, June 6). Viking Lander 1 Binned and Splined data . Retrieved from http://www-k12.atmos.washington.edu/k12/mars/data/vl1/part1.html.
[38] PDS Atmospheres Node. (n.d.). Retrieved 2022, from https://pds-atmospheres.nmsu.edu/PDS/data/PDS4/InSight/twins_bundle/.
[39] NASA. (n.d.). *Mars fact sheet*. NASA. Retrieved May 29, 2022, from https://nssdc.gsfc.nasa.gov/planetary/factsheet/marsfact.html
[40] Office of Energy Efficiency & Renewable Energy, Walker, A., & Desai, J., Understanding Solar Photovoltaic System Performance3–13 (2021). U.S. Department of Energy.
[41] Gaier, J. R., & Perez-Davis, M. E. (1994). In *The viability of photovoltaics on the Martian surface*. Washington, DC; National Aeronautics and Space Administration.
[42] Mason, L. S. (2018). A comparison of energy conversion technologies for Space Nuclear Power Systems. *2018 International Energy Conversion Engineering Conference*. https://doi.org/10.2514/6.2018-4977
[43] Gibson, M. A., Oleson, S. R., Poston, D. I., & McClure, P. (2017). NASA's Kilopower reactor development and the path to higher power missions. *2017 IEEE Aerospace Conference*. https://doi.org/10.1109/aero.2017.7943946
[44] Gibson, M. A., Poston, D. I., McClure, P., Godfroy, T., Sanzi, J., & Briggs, M. H. (2018). The Kilopower reactor using Stirling Technology (Krusty) Nuclear Ground test results and lessons learned. *2018 International Energy Conversion Engineering Conference*. https://doi.org/10.2514/6.2018-4973
[45] *Martian Seasons and Solar Longitude*. (n.d.). Retrieved 2022, from http://www-mars.lmd.jussieu.fr/mars/mars.html
[46] Hartwick, V. L., Toon, O. B., Lundquist, J. K., Pierpaoli, O. A., & Kahre, M. A. (2022). Assessment of Wind Energy Resource Potential for future human missions to Mars. Nature Astronomy. https://doi.org/10.1038/s41550-022-01851-4
[47] De, S. (2017). Weebles only wobble but eggs fall down. *Mathematics Magazine*, *90*(2), 99–107. https://doi.org/10.4169/math.mag.90.2.99

V. Appendix

V.1 Energy System

The following section discusses possible energy alternatives for use on Mars. Further in-depth wind data can also be found in the section below.

V.1.A Solar Cells

Traditional solar cells were originally considered a possible energy source for the aircraft. However, due to current technological limitations in solar cell technology as well as reduced solar flux on mars, it was determined that the use of traditional solar panels would be insufficient. The maximum solar irradiance on Mars is 586.2 W/m2 [39], which is approximately 43.1% of that of Earth's conditions. A preliminary study on the use of traditional solar panels was conducted. Using historical solar cell

performance data acquired from the United States Department of Energy (DOE), an efficiency of 25% and a performance ratio of .2 were selected [40]. With these values, it was calculated that a total solar cell area of 3,411.8 sqm would be necessary to produce 100 kW. These preliminary results show that the use of traditional solar cells would not be a sufficient solution for the energy ecosystem. Thus, it was concluded that more efficient energy systems needed to be considered and researched.

When considering the use of solar cells, environmental trends and conditions must be considered. Various viability studies have been conducted to test the feasibility of photovoltaics (PVs) on the Martian surface. Using the Martian Surface Wind Tunnel (MARSWIT) at NASA, there have been several comprehensive tests performed to better understand how dust composition, particle size, wind velocity, and angle of attack can affect PVs. Using Viking 1's soil compositional readings, a study analyzed the effect of Martian dust storms on PVs, showing that the threshold clearing velocity would occur at 22 m/s [41]. Within this wind tunnel test, it was also concluded that significant abrasion of the PVs would occur at high velocities of wind (starting at 85 m/s) [41]. These preliminary results show promising data in reference to the durability of solar cells in a Martian environment, as wind speeds of 85 m/s are much higher than historical wind speed data recorded by the Viking 1 rover. However, because of the high threshold clearing velocity for the dust composition, Solar cells would require constant maintenance and cleaning. Martian dust particles are small and have slight electrostatic properties, making them likely to stick to surfaces. Dust particles covering PVs limit the amount of sunlight reaching the cells, and in turn, decrease energy production. This could potentially pose many issues as the area of PVs required for nominal power energy production is very large. Daily human maintenance with such a large area would not be possible and further technological development would need to occur to make the maintenance process efficient. The cost and time necessary to maintain solar cells under Martian conditions were deemed unreasonable in comparison to expected energy and power outputs.

V.1.B. Surface Fission Station

Nuclear energy is a powerful source of energy that can be used during adverse climate conditions on Mars. In the absence of sufficient solar irradiance or wind speeds, nuclear energy stations can be a reliable source of energy. Various Lunar and Martian rovers have utilized this technology, showing that the use of nuclear fission has significant potential to power larger mobility systems in the future[42]. Two major forms of nuclear energy sources have been historically used under compromised environmental conditions, including radioisotope power systems (RPSs) and fission power systems (FPSs). RPSs rely on the natural decay heat from Plutonium (Pu) to generate electricity. Various NASA missions have utilized this form of nuclear energy including the Viking and Mars curiosity rover, showing that the use of this technology is possible under Martian conditions. Historical trends and laboratory testing show that RPSs have the potential to only generate approximately $1kW$ of electric power [42,43], which can be considered insufficient in the context of the needs necessary for the Martian transportation and energy ecosystem. FPSs function through the sustained fission reaction of Uranium (U). In comparison to RPSs, FPSs can produce power outputs ranging from kilowatts to megawatts, showing a stark improvement in electric power production. Despite more favorable electric power outputs, FPSs have not been used at the same magnitude as RPSs due to technological limitations. Needs for novel material testing and reactor fuel are among some of the many reasons why the development of FPSs systems has been limited in the past. Over the past few decades, NASA has been developing Fission system projects. The most notable to consider is the Killopower project which aimed to allow for 1-10 kilowatt-electric (kWe) production. With NASA's recent partnership with the DOE's National Nuclear Security Administration, significant strides have been made

in the development of a successful fission power station. Ground testing with both depleted uranium (DU) has been completed to verify the feasibility of a non-nuclear design prior to nuclear testing [43]. The Kilopower station then underwent further testing with a highly enriched uranium (HEU) core. The testing of the Kilopower Reactor Using Stirling Technology (KRUSTY) was completed in 2018. The testing procedures verified that the KRUSTY reactor dynamics could withstand both nominal and off-nominal mission scenarios [44]. Verifying that efficiency and safety could be maintained under unexpected conditions. As further testing is completed, more information can be collected on a fission reactor's feasibility as an energy source for the Martian ecosystem. From the test, it was concluded that the reactor can successfully regulate the reactor core temperature through various simulated nominal and off-nominal scenarios while operating at steady state with a thermal power output of $4kW$ at a temperature of 800 degrees Celsius [44].

Further NASA research and development has led to future plans to create a fission station that can reliably produce $10kW$ per system. The Fission Solar power station (as proposed by NASA) will be the primary source of energy for the aircraft. These surfaces come in pairs of 4, each generating 10kW of energy ($40kW$ per setup). This is enough to run 30 households for 10 years continuously. Thus, to obtain $200kW$ we need approximately 5 systems of fission surfaces. A surface power system for space, unlike terrestrial reactors, must endure the extreme vibration stresses experienced during launch or landing on a planet's surface. The units will be structurally strong to protect the coolant, reactor core, and electronic control systems, as well as the support system that keeps it all together, to achieve this. The DOE released a Request for Proposals in 2021, in collaboration with NASA, seeking design proposals for a fission surface power system that might be ready to fly within a decade for a demonstration on the Moon. It is important to note, when considering the use of nuclear energy in conjunction with human habitation, it is important to carefully examine possible adverse health effects that may occur [46]. Possible hazardous conditions pose significant limitations when considering the design of a nuclear energy powered habitat. With further research Surface Fission Stations might be a viable option to power the eVTOL aircraft and Martian habitat in the future.

V.2 Further Wind Analysis

A Wind speed and pattern analysis was also completed for the landing spot of Elysium [38]. Due to the significant difference in wind reading analysis methodology, it was decided to leave the derived Elysium data out of the initial wind energy analysis. However, the results found still have significant implications on our understanding of wind patterns on mars and is thus included in the appendix. The Elysium wind data was received from the Insight rover [38]. Insight recorded wind speed data every few seconds. Due to this high frequency in data collection, it was not possible to complete a comprehensive energy production analysis as is seen done with the Chryse and Utopia landing sites. The table below shows sample energy calculations done on individual days. Due to a high amount of raw data points, the analysis had to be done by averaging every wind speed recorded per day to an average daily windspeed. With the daily wind speed values found, the average daily power and energy outputs are calculated. The following table illustrates the average daily wind speeds (with he $1/7^{th}$ power rule applied) as well as the average daily, weekly, and monthly energy production values.

Elysium Wind Analysis	
Average Wind Speed (m/s)	6.28
Average Daily Energy Production (kWh)	2.16
Average Weekly Energy Production (kWh)	14.93
Average Monthly Energy Production (kWh)	56.52

Table 10. Elysium Wind Analysis Results

Despite having a different wind energy analysis methodology, the results agreed well with those found in the Chryse and Utopia landing sites. There is a lot of value in the abundance of data found on wind speeds on Elysium. With appropriate software, this data can yield very valuable and accurate information concerning wind patterns on Mars. A comparison between the average wind speeds of the three discussed landing sites can be found in the table below. The wind speeds denoted are calculated using the published data and with the $1/7^{th}$ power rule applied.

Average Wind Speed Comparisons	
Elysium (m/s)	6.28
Chryse (m/s)	4.75
Utopia (m/s)	5.04
Average (m/s)	5.36

Table 11. Landing Sites Average Wind Speed

V.3 Further Wind Turbine Design Considerations

The proposed wind turbine design is comprised of a hub at 20 meters height, with a blade radius of 5 meters. With the proposed rocket having a payload fairing with an extended height of 22 meters, this configuration should allow for full assembly transportation. This design parameter would facilitate the installation of these turbines without the need for a team of humans or robots to assist in the assembly. A proposed solution for the wind turbine assembly is to make the design statically stable at the base. This design would allow for the wind turbine to be released from the payload fairing at a lower atmosphere via parachutes. With a statically stable base, when landing the wind turbine should have the ability to stabilize itself independent of any need for additional installation or assembly. The proposed wind turbine base design is modeled after the "Weeble Wobble" toys. These structures possess a low center of gravity that allows for static stability- making it so that in the presence of external forces the toys can independently stabilize to an upright position. This base design allows for static stability due to the following principle: The equilibrium of an object will be stable if the vertical height of the center of mass (at the equilibrium position) is smaller than the radius of curvature for the contour of the object [47]. The design of the base is dependent on the materials and overall mass distribution of the designed wind turbine and is thus subject to change. To further stabilize the base of the wind turbine after landing, a proposed solution is to use Martian soil to fill the base of the wind turbine to eliminate any movement due to changing wind speeds or directions.

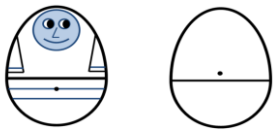

Figure 7. Weeble Wobble Toy Stable Equilibrium Condition [47]